

# Spermatogenesis and sperm structure of *Neopanorpa lui* and *Neopanorpa lipingensis* (Mecoptera: Panorpidae) with phylogenetic considerations

BEI-BEI ZHANG<sup>1,2</sup> & BAO-ZHEN HUA<sup>\*,1</sup>

<sup>1</sup> State Key Laboratory of Crop Stress Biology for Arid Areas, Key Laboratory of Plant Protection Resources and Pest Management, Ministry of Education, College of Plant Protection, Northwest A&F University, Yangling, Shaanxi 712100, China — <sup>2</sup> Institute of Tropical Agriculture and Forestry, Hainan University, Danzhou, Hainan 571737, China; Bao-Zhen Hua\* [huabzh@nwafu.edu.cn]; Bei-Bei Zhang [zhangbeibei@nwafu.edu.cn] — \*Corresponding author.

Accepted 21.vi.2017.

Published online at [www.senckenberg.de/arthropod-systematics](http://www.senckenberg.de/arthropod-systematics) on 11.xii.2017.

Editors in charge: Ulrike Aspöck & Klaus-Dieter Klass

## Abstract

Spermatogenesis and sperm ultrastructure were investigated in *Neopanorpa lui* Chou & Ran and *Neopanorpa lipingensis* Cai & Hua by light and transmission electron microscopy. Two lateral lamellae run along the lateral grooves of the spermatid nucleus during spermiogenesis, but disappear in the mature spermatozoa. Sperm cells are very similar in ultrastructure between the two species. The spermatozoa are elongated cells, each comprising an apical bilayered acrosome inserted on the anterior nuclear region, an elongate nucleus that occupies the anterior sperm region, a neck region, and a posterior long flagellum. The nucleus has two prominent lateral grooves and assumes a helical appearance. The flagellum is helical and consists of a 9+2 axoneme, two mitochondrial derivatives of unequal size, one accessory body, and two extra-axonemal accessory structures. The uniqueness of spermatozoa of *Neopanorpa* lies in the specifically spoon-shaped larger mitochondrial derivative along most of the flagellum length. A tentative phylogenetic analysis based on sperm structure supports a possible monophyletic clade comprising Panorpidae, Panorpididae, Bittacidae, and Boreidae of Mecoptera with two non-homoplasious characters: glycocalyx organised in longitudinal ridges and two extra-axonemal accessory structures/rods in flagellum. Closer affinities of Siphonaptera and the mecopteran clade are suggested by the characters of two asymmetric mitochondrial derivatives and the presence of mitochondrial derivative with crystalline structure. The sister group relationship of Panorpidae with Panorpididae is supported by the presence of nuclear fiber and the irregular shape of the larger mitochondrial derivative.

## Key words

Insecta, mitochondrial derivative, *Neopanorpa*, phylogeny, spermatozoa, spermiogenesis.

## 1. Introduction

Mecoptera, a minor order in Antliophora of holometabolous insects, is unique in Holometabola because most mecopteran groups (especially Panorpidae, Nannochoiristidae, Choristidae, and Bittacidae) possess a pair of prominent compound eyes in their larval stages (BYERS & THORNHILL 1983; MELZER et al. 1994; KRISTENSEN 1999; CHEN et al. 2012). Its relationship with Siphonaptera and

Diptera, however, has not been satisfactorily clarified in Antliophora (WILLMANN 1987; WHITING 2002; BEUTEL & BAUM 2008; WIEGMANN et al. 2009; BEUTEL et al. 2011; FRIEDRICH et al. 2013; MISOF et al. 2014). WHITING (2002) assumed that Mecoptera (Boreidae) is paraphyletic with respect to Siphonaptera based on molecular data. BEUTEL & BAUM (2008) considered the peculiar family Nanno-

choristidae of Mecoptera as the sister group of Diptera supported by the mouthpart structure of adults. FRIEDRICH et al. (2013) also proposed that Mecoptera is a paraphyletic group based on morphological characters of the adult head. However, some researchers (WILLMANN 1987; WIEGMANN et al. 2009; MISOF et al. 2014) argued that Mecoptera is monophyletic as the sister group of Siphonaptera. BEUTEL et al. (2011) even regarded Mecoptera as the sister group of Diptera and Siphonaptera based on morphological data. Additional characters are obviously needed to solve the phylogenetic position problem of Mecoptera. The ultrastructure of spermatozoa might partly fulfill this requirement.

Spermatozoa are highly specialized cells, characterized by patterns of rapid and divergent morphological evolution (BIRKHEAD et al. 2009; DALLAI et al. 2016; GOTTARDO et al. 2016). The variation in sperm morphology, especially the ultrastructure, can provide valuable characters for the assessment of evolution and the reconstruction of phylogeny in various groups (JAMIESON 1987; JAMIESON et al. 1999; DALLAI 2009, 2014; DALLAI et al. 2016; GOTTARDO et al. 2016). The ultrastructure of spermatozoa has been extensively studied in the vast number of species of insects (BACCETTI 1972; JAMIESON 1987; JAMIESON et al. 1999; DALLAI 2014; DALLAI et al. 2016). However, sperm structure is still poorly documented in Mecoptera to date, and only four species have been investigated in Panorpidae (GASSNER et al. 1972; JAMIESON et al. 1999; DALLAI et al. 2003; ZHANG et al. 2016); two species in Bittacidae (SHEPARDSON et al. 2014); two species in Boreidae (DALLAI et al. 2003; RUSSELL et al. 2013); and one species in Panorpididae (ZHANG & HUA 2014).

Panorpidae, the largest family of Mecoptera, comprises approximately 400 extant species, which are distributed throughout Asia, North America, and Europe (KALTENBACH 1978; PENNY & BYERS 1979; BYERS & THORNHILL 1983; HU et al. 2015). The species of Panorpidae are currently assigned to seven genera: *Panorpa* Linnaeus, 1758; *Leptopanorpa* MacLachlan, 1875; *Neopanorpa* Weele, 1909; *Sinopanorpa* Cai & Hua, 2008; *Furcatopanorpa* Ma & Hua, 2011; *Dicerapanorpa* Zhong & Hua, 2013; and *Cerapanorpa* Gao, Ma & Hua, 2016. Previous sperm structure studies of Panorpidae (GASSNER et al. 1972; JAMIESON et al. 1999; DALLAI et al. 2003; ZHANG et al. 2016) only dealt with species of *Panorpa* and *Furcatopanorpa*, the sperm ultrastructures of which are distinctly different in the mitochondrial derivative of flagellum, whereas the second largest genus *Neopanorpa* has not been involved.

In this study, we investigated the spermatogenesis and sperm ultrastructure of *Neopanorpa lui* Chou & Ran, 1981 and *Neopanorpa lipingensis* Cai & Hua, 2009 by light and transmission electron microscopy, in order to provide eventual additional characters for future phylogenetic analysis of Panorpidae, and in an attempt to elucidate the phylogenetic relationships of Mecoptera in Antliophora.

## 2. Material and methods

### 2.1. Insect collection

Adult males of *Neopanorpa lui* Chou & Ran, 1981 were obtained from the Tiantaishan National Forest Park (34°13'N 106°59'E, elev. 1500–1600 m) in the Qinling Mountains, Shaanxi Province from late June to early July in 2014 and mid-July in 2015. Adult males of *Neopanorpa lipingensis* Cai & Hua, 2009 were collected at Huanglongtan (31°53'N 109°31'E, elev. 900–1000 m) in the Hualong Mountains, Shaanxi Province in mid-July 2015.

### 2.2. Light microscopy

Live adult males were anaesthetized with diethyl ether, and their testes and epididymids were rapidly dissected in Ringer's solution under a Nikon SMZ1500 stereo microscope (Nikon, Tokyo, Japan). The testicular follicles were opened at the basal part and the sperm bundles were spread onto clean microslides. Pictures were taken with a QImaging Retiga 2000R Fast 1394 Digital CCD equipped on the microscope. To determine the size of sperm nucleus, some slides were stained with 4,6-diamino-2-phenylindole (DAPI, Beyotime) for 5 min, and washed in distilled water. Photographs were taken with a Nikon DS-R1 digital camera attached to a Nikon Eclipse 80i epifluorescence microscope (Nikon, Tokyo, Japan).

For histological observation, the samples embedded in polymerized Epon 812 resin were cut into semi-thin sections with a Leica EM UC7 ultramicrotome (Leica, Nussloch, Germany), stained with 0.5% toluidine blue, and examined under the microscope.

### 2.3. Transmission electron microscopy

The testes and epididymides of live male adults were dissected rapidly in Ringer's solution and fixed at 4°C overnight in a mixture of 2% paraformaldehyde and 2.5% glutaraldehyde in 0.1 M phosphate buffer (PB, pH 7.2), in which 3% sucrose was added.

The fixed samples were rinsed six times with PB, and post-fixed in phosphate-buffered 1% osmium tetroxide (OsO<sub>4</sub>) for 1.5 h at 4°C. After rinsing six times with PB, the testicular follicle and epididymis samples were dehydrated in a graded series of acetone (30%, 50%, 70% for 10 min each, 80% for 15 min, 90% for 20 min, and 100% for 30 min twice), infiltrated successively with three mixtures of acetone/Epon 812 resin (3:1 for 2 h, 1:1 for 4 h, and 1:3 for 12 h) and pure Epon 812 resin for 24 h twice at room temperature, and were embedded in pure Epon 812 resin, polymerized at 30°C for 24 h and at 60°C 48 h.

Ultra-thin sections were cut with a diamond knife on the ultramicrotome, double stained with uranyl acetate and lead citrate for 10 and 8 min, respectively, and ex-

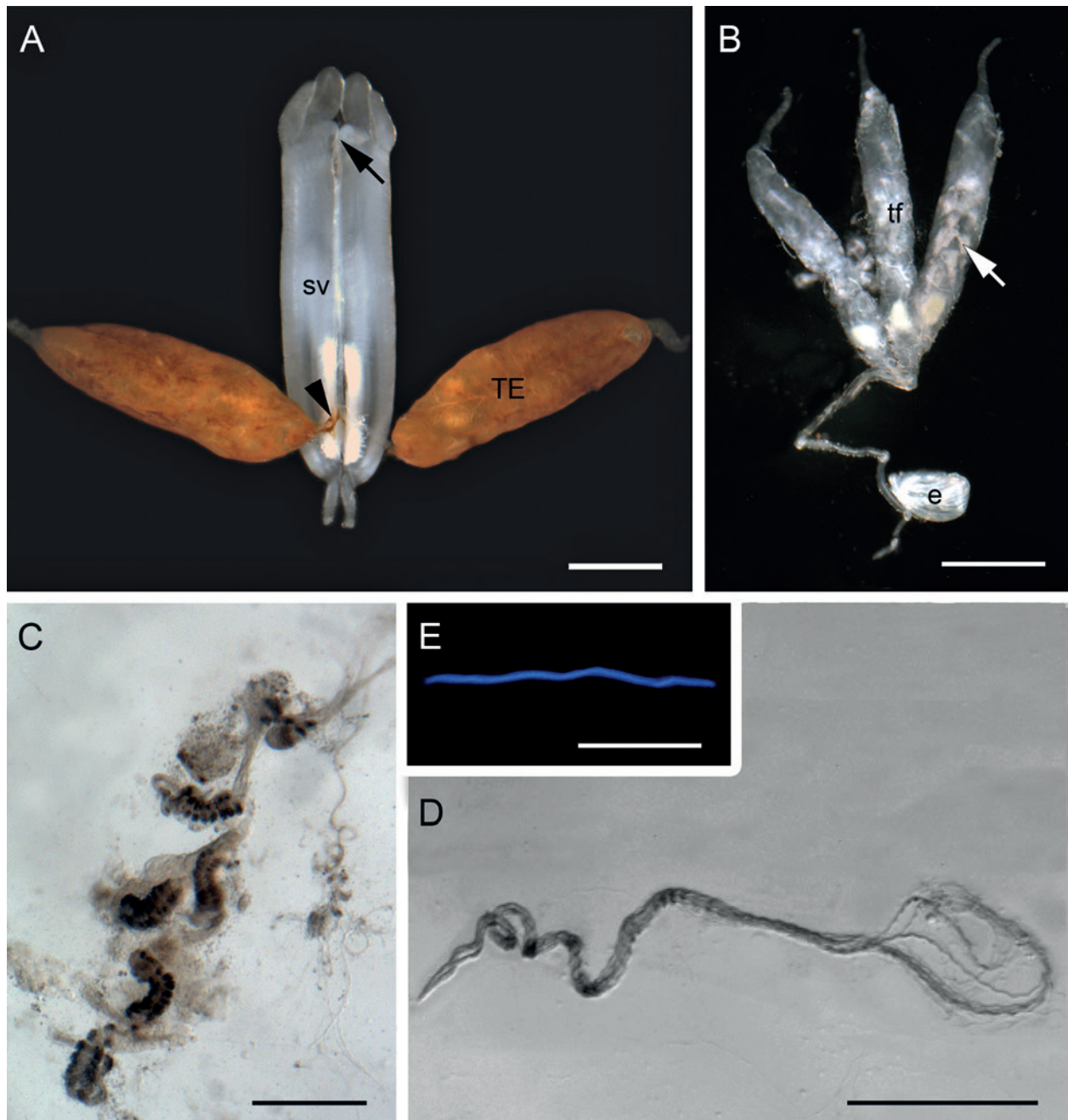


**Fig. 1.** *Neopanorpa lui* Chou & Ran, 1981: male reproductive organs and sperm bundles, light micrographs. **A:** Testis-epididymis complex (TE), vas deferens (arrowhead), and seminal vesicle (sv); arrow points to the entry of the vas deferens entering the seminal vesicle. **B:** Testis-epididymis complex consisting of three testicular follicles (tf) and an epididymis (e), arrow points to sperm bundles. **C:** Sperm bundles in a testicular follicle. **D:** A sperm bundle. **E:** The sperm nucleus stained with DAPI. (Scale bars: A, B: 0.5 mm; C, D: 0.2 mm; E: 10  $\mu$ m)

amed under a Hitachi HT7700 transmission electron microscope (Hitachi, Tokyo, Japan) at 80 kV.

## 2.4. Phylogenetic analyses

Phylogenetic analyses were conducted using maximum parsimony in TNT version 1.5 (GOLOBOFF et al. 2008) with 1000 random addition traditional searches and NONA 2.0 (GOLOBOFF 1999) using heuristic searches with 1000 replications. Micropterigidae and Hepialidae in Lepidoptera were used as outgroup taxa. All taxa of

Antliophora were treated as ingroup members, including Chironomidae and Limoniidae in Diptera (selected the relative basal taxa), Pulicidae in Siphonaptera (the only one family studied), and four studied families (Bitacidae, Boreidae, Panorpidae, and Panorpididae) in Mecoptera. Twenty-two characters (0, plesiomorphic state; 1 or 2, apomorphic states; [01/02/012], polymorphic characters; ?, missing or unknown; -, gap) of sperm ultrastructure (see section 3.4.) were coded in a data matrix (Table 1). Some characters were extracted from previous studies (e.g., HAMON & CHAUVIN 1992; JAMIESON et al. 1999; DALLAI et al. 2003, 2007, 2008; RUSSELL et



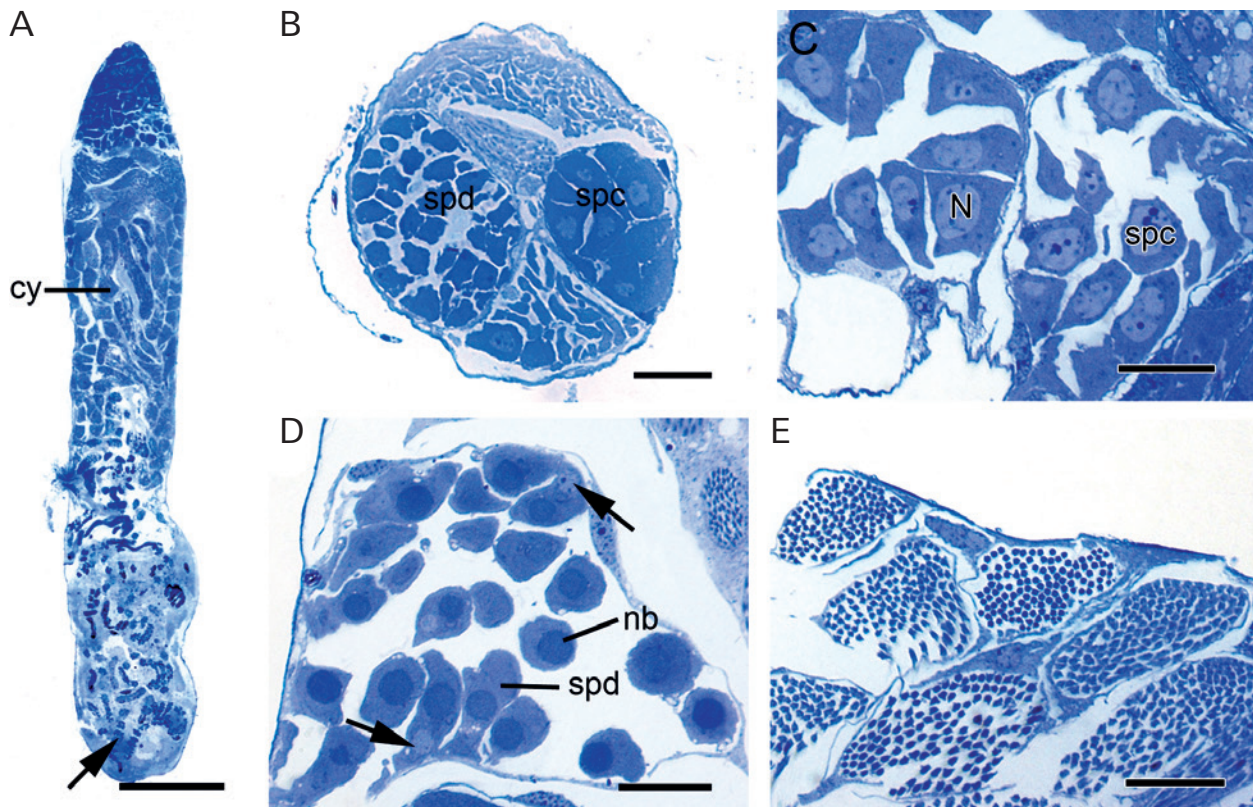


**Fig. 2.** *Neopanorpa lui* Chou & Ran, 1981: testicular follicle, sperm cyst, histological micrographs. **A:** Longitudinal section of a testicular follicle with cysts (cy) and sperm bundles (arrow). **B:** Cross-section of the distal region, showing different cysts with spermatocytes (spc) and spermatids (spd), respectively. **C:** Magnification of spermatocytes (spc) with nucleus (N). **D:** Spermatids (spd) in a cyst characterized by small nuclei (arrows) and conspicuous nebenkerns (nb). **E:** Magnification of cysts. (Scale bars: A: 100  $\mu$ m; B–E: 20  $\mu$ m)

al. 2013; SHEPARDSON et al. 2014; ZHANG & HUA 2014; ZHANG et al. 2016; GOTTARDO et al. 2016). All characters were initially equally weighted. Bremer support value or decay index (BREMER 1994) for the resultant strict consensus tree was calculated with TNT. The unambiguous characters were mapped on the tree using WinClada version 1.00.08 (NIXON 2002).

### 3. Results

#### 3.1. Gross morphology of the male testes

The males of *Neopanorpa* each have a pair of long elliptical testes (Fig. 1A). Each testis consists of three translucent testicular follicles (~1.8 mm in length and 0.25 mm in diameter) (Fig. 1B), which open into the long vas deferens. The vas deferens is highly coiled at the distal part to form an epididymis, which is pressed against the lateral base of the testis. The testis and epididymis are enclosed together by a common brown peritoneal sheath, forming a testis-epididymis complex (Fig. 1A). The vas deferens runs forward along the meso-ventral line of the paired well-developed subcylindrical seminal vesicles after leaving the peritoneal sheath, and enters the seminal vesicles at the anterior end of the latter (Fig. 1A).

In the sexually mature males, spermatozoa are formed in the testicular follicles and temporarily stored in the epididymides before their transfer to the reproductive tract of the female. The testicular follicle is made up of an epithelium lying on the basal lamina surrounded by a thin muscular layer, and numerous cysts (Figs. 2A, 3A). In the cytoplasm of epithelial cells are a series of vesicles, numerous mitochondria, extensive rough endoplasmic reticulum, and some multilamellar bodies (Fig. 3A). The produced spermatids undergo a series of distinct transformations in the testicular follicles (Figs. 3D,F,G, 4A–C), and eventually form spermatozoa. The spermatozoa are held together in the form of coiled sperm bundles of approximately 1100  $\mu$ m in length (Fig. 1C,D) before transfer to the epididymides. The epididymis is composed of a fairly thick epithelium, a basal lamina, and a layer of circular smooth muscles externally (Fig. 5A,B). Vesicles and mitochondria are abundant in the cytoplasm of epithelial cells, whose apical surface facing the lumen has numerous microvilli (Fig. 5B).

#### 3.2. Spermatogenesis and sperm ultra-structure of *Neopanorpa lui*

Spermatogenesis progresses in cysts within the testicular follicle. At the distal region of the testicular follicle, some cysts are filled with spermatocytes, and others with



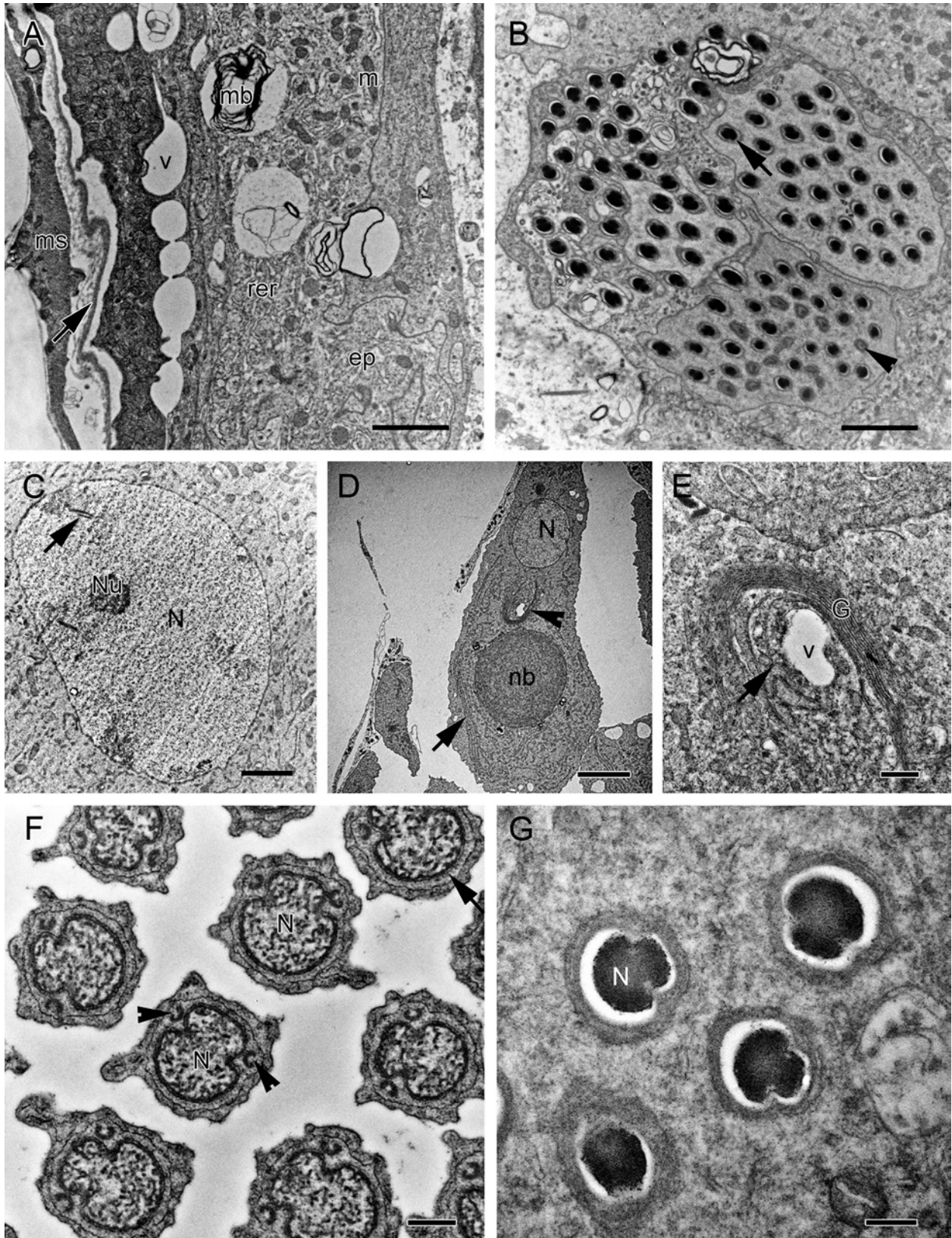


**Fig. 3.** *Neopanorpa lui* Chou & Ran, 1981: testicular follicle and spermatogenesis, TEM micrographs. **A:** Longitudinal section of the wall, showing the muscular layer (ms), basal lamina (arrow), and epithelium (ep). Vesicles (v), mitochondria (m), rough endoplasmic reticulum (rer), and multilamellar bodies (mb) are visible in the epithelial cells. **B:** Cross-section at the head region of the sperm bundle in a cyst, showing nucleus (arrow) and acrosome (arrowhead). **C:** A spermatocyte nucleus (N) with the nucleolus (Nu) and synaptonemal complex (arrow). **D:** A spermatid with the nucleus (N), nebenkern (nb), Golgi apparatus together with pro-acrosomal material (arrowhead), and endoplasmic reticulum (arrow). **E:** Magnification of the pro-acrosomal material (arrow) with a distinct vesicle (v) along the concave side of the Golgi apparatus (G). **F:** Lateral laminae (arrowheads) alongside the lateral grooves of the nucleus (N) during spermiogenesis; arrow points to microtubules. **G:** Nucleus (N) with condensed chromatin in the nearly mature stage. (Scale bars: A–C: 2  $\mu$ m; D: 4  $\mu$ m; E, F: 0.5  $\mu$ m; G: 0.2  $\mu$ m)



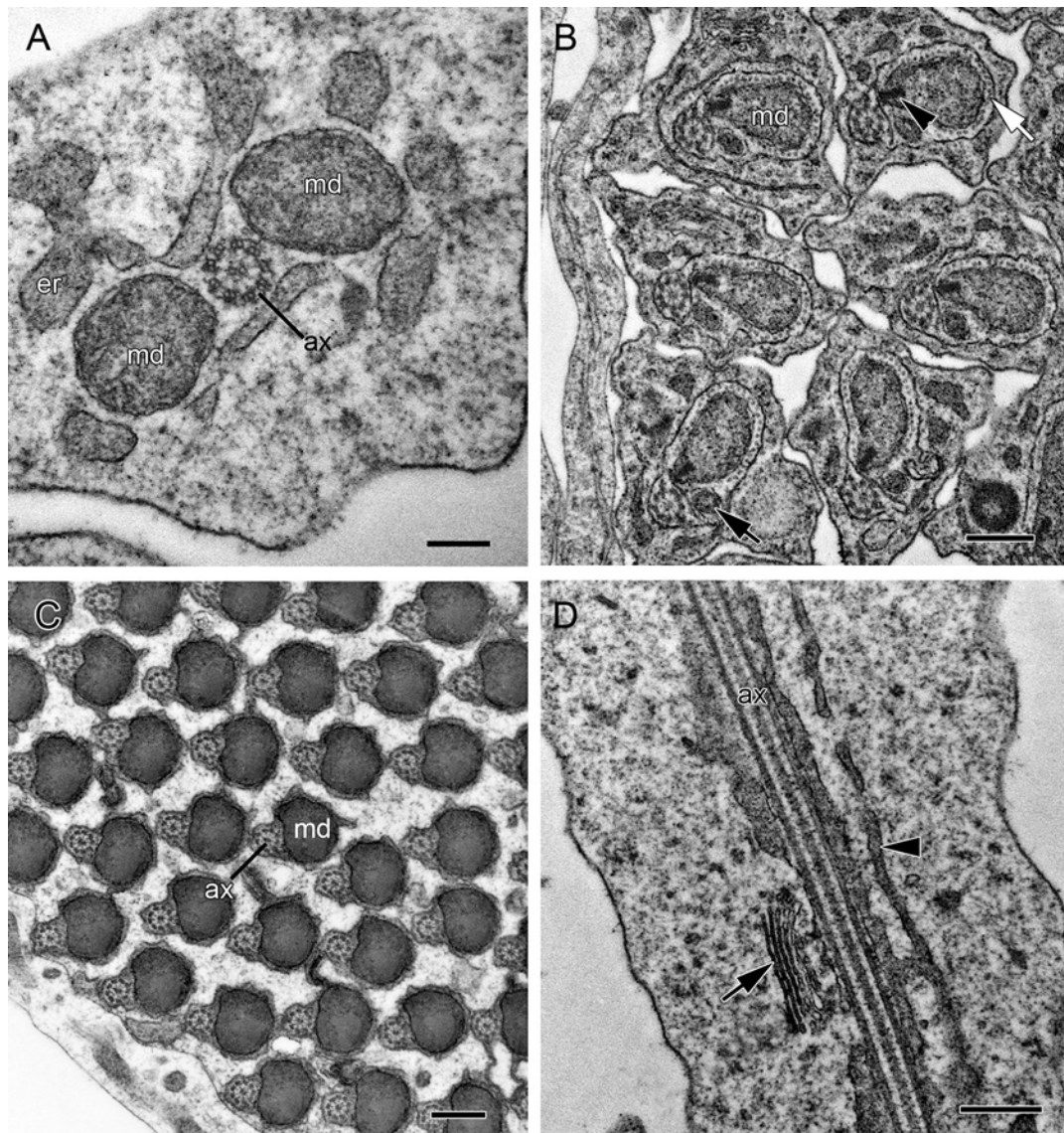


**Fig. 4.** *Neopanorpa lui* Chou & Ran, 1981: spermatids and flagellum, TEM micrographs. **A:** Cross-section of the early spermatids, showing a 9+2 axoneme (ax), endoplasmic reticulum (er), and two mitochondrial derivatives (md). **B:** Flagellum with two mitochondrial derivatives of unequal size: the larger one (md) with a crystalline body (arrowhead) surrounded by microtubules (white arrow); arrow points to the smaller one. **C:** Cross-section of the flagellum of late spermatids, showing an axoneme and the larger mitochondrial derivative (md). **D:** Longitudinal section of the axoneme of early spermatids, showing the axoneme (ax), endoplasmic reticulum (arrowhead), and Golgi apparatus (arrow). (Scale bars: A: 0.2  $\mu$ m; B–D: 0.5  $\mu$ m)

spermatids (Fig. 2B). In each cyst, a spermatogonium undergoes seven successive divisions, eventually generating 128 spermatids (Fig. 3B), which later transform into elongate spermatozoa and further into a sperm bundle through shape deformation. Each cyst contains germ cells of the same maturation stage (Fig. 2B,E). A series of cysts of primary spermatocytes are progressively displaced in an increasing order of maturation from the apical to the basal portion in the whole testicular follicle (Fig. 2A).

The spermatocytes are recognized by the presence of a synaptonemal complex in their nucleus. The nucleus of the spermatocyte is approximately 12.6  $\mu$ m in diameter with uniformly diffuse chromatin (Figs. 2C, 3C). The spermatids are roughly globular, approximately 14  $\mu$ m in diameter (Fig. 2D). The early spermatids each are pro-

vided with a rounded nucleus characterized by homogeneously diffuse chromatin of 5.3  $\mu$ m in diameter, a conspicuous “nebenkern” consisting of fused interlocked mitochondria, and a Golgi apparatus whose concave side faces the nucleus (Fig. 3D). The pro-acrosomal material is present in the fossa of the Golgi apparatus (Fig. 3D,E). Endoplasmic reticulum is also visible in the cytoplasm (Fig. 3D, arrow).

During the spermiogenesis the spermatids undergo a distinct transformation, changing from spheroid in shape to an elongated appearance. With the transformation of nuclei the chromatin condenses gradually with the increase of its electron density (Fig. 3F,G). Two lateral laminae accompany the spermatid nucleus alongside the two lateral grooves of nuclear envelope (Fig. 3F) and extend along the entire length of sperm head to the cen-



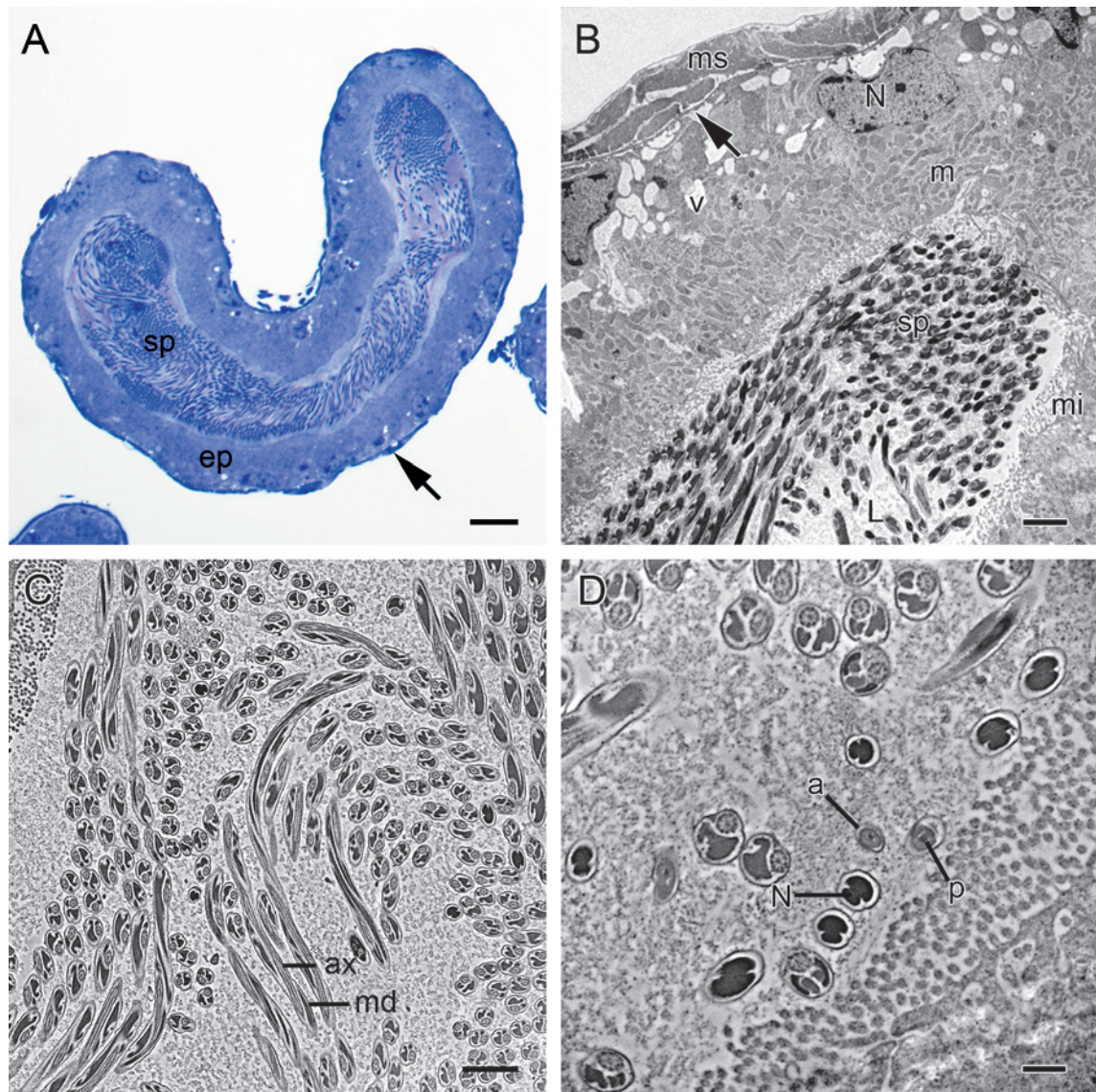


**Fig. 5.** *Neopanorpa lui* Chou & Ran, 1981: epididymis, spermatozoa, histological (A) and TEM (B–D) micrographs. **A:** Longitudinal section of an epididymis, showing the muscular layer (arrow), epithelium (ep), and lumen filled with spermatozoa (sp). **B:** Cross-section of epididymis, showing muscular layer (ms), basal lamina (arrow), epithelial cells with numerous apical microvilli (mi) projecting into the lumen (L), mitochondria (m) and vesicles (v). **C,D:** Spermatozoa in the lumen, showing the helical array of axoneme (ax) and mitochondrial derivatives (md) in longitudinal section, the bilayered acrosome (a) with the central perforatorium (p), and mushroom-shaped nucleus (N) in cross-section. (Scale bars: A: 10  $\mu$ m; B, C: 2  $\mu$ m; D: 0.5  $\mu$ m)

triolar region. A layer of singlet microtubules encircles the nucleus and lateral laminae. The lateral lamellae, however, exist only in the spermatids, and vanish in the spermatozoa.

The two mitochondrial derivatives are almost of equal size in the early spermatids (Fig. 4A). One mitochondrial derivative, however, diminishes evidently in later stages. It is evident that the larger mitochondrial derivative is surrounded by a layer of singlet microtubules (Fig. 4B). Approaching the mature stage, only a single elliptical mitochondrial derivative remains in the most length of the flagellum (Fig. 4C). A notable feature of the mitochondrial derivative lies in the drop-shaped crystalline body facing the axoneme (Fig. 4B). The axoneme has a 9+2 microtubular pattern: nine doublet microtubules with dynein arms and thick radial spokes, and two central micro-

tubules. Along the axoneme run endoplasmic reticulum and Golgi apparatus in the early spermatid stage (Fig. 4D).

The mature spermatozoa are elongated and filiform, each consisting of a short head, a neck transition region, and a long posterior flagellum (Fig. 6). The head comprises an apical conical acrosome and a nucleus (Fig. 7B). The acrosome is approximately 0.22  $\mu$ m in diameter at the base and is bilayered, consisting of an outer acrosomal vesicle and a central perforatorium (Fig. 7B).

The sperm nucleus is elongated, measuring 25  $\mu$ m in length (Fig. 1E). The nucleus has two lateral grooves along its whole length and is mushroom-shaped in cross-section (Fig. 5D). The nucleus assumes a helical shape in longitudinal section (Fig. 7A), and contains a series of parallel-spaced septa in the groove. The aforementioned

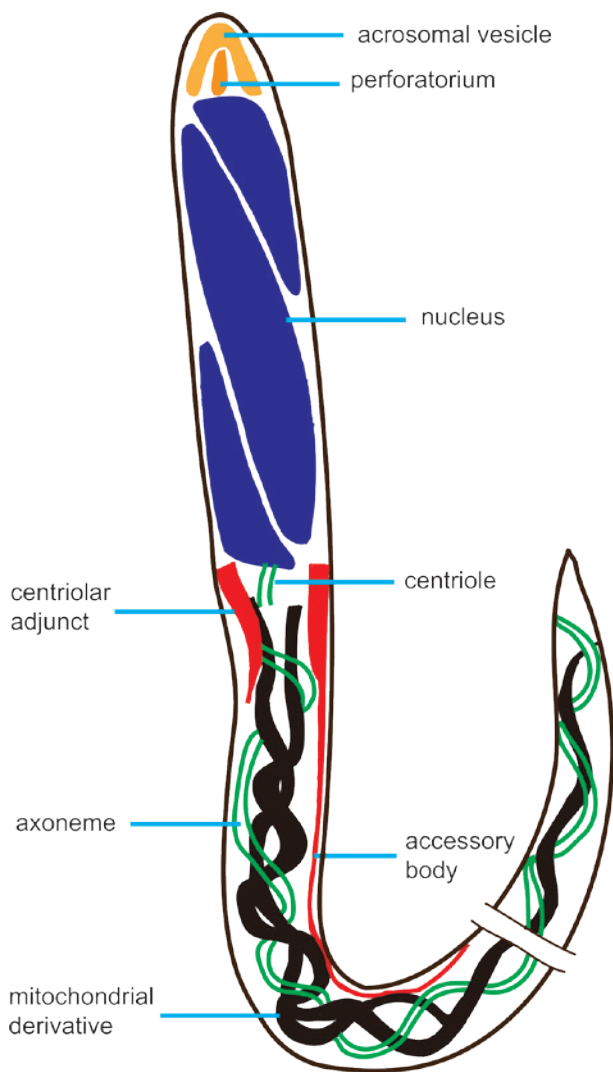


**Fig. 6.** Schematic drawing illustrating the sperm morphology of *Neopanorpa lui*.

lateral laminae, which once run along the nucleus during the spermiogenesis, are absent in the mature spermatozoa (Fig. 7F,G).

The neck region consists of a centriole and the centriolar adjunct material. The centriole usually inserts into one side of the posterior extremity of the nucleus (Fig. 7C,D). Beneath the centriole is the electron-dense centriolar adjunct. The centriolar adjunct is well-developed on the periphery, assuming the shape of a characteristic sheath (Fig. 7A,D,F), and gradually diminishes along the flagellum.

The flagellum is very long and composed mainly of an axoneme, two mitochondrial derivatives, one accessory body, and two extra-axonemal accessory structures. The axoneme and mitochondrial derivatives are arranged in a helicoidal array (Fig. 5C). The axoneme has, along the most length of the flagellum, a regular pattern of 9+2 microtubules, which become disorganized in the terminal part (Fig. 7E). The extra-axonemal accessory structure

is thin, and located longitudinally between the axoneme and the mitochondrial derivative.

The two mitochondrial derivatives differ from each other in diameter and length, although they are almost identical in size at the basal part of the flagellum within the neck region (Fig. 7D). Along the flagellum one mitochondrial derivative gradually diminishes, and eventually disappears with only one mitochondrial derivative retained in the remaining length of the flagellum (Figs. 5D, 7F). The remained mitochondrial derivative assumes a spoon shape in cross-section (Fig. 5D). At the terminal region of the flagellum, the longer mitochondrial derivative becomes roughly elliptical in cross-section, with its diameter decreased ( $\sim 0.2 \mu\text{m}$ ) (Fig. 7E).

### 3.3. Sperm ultrastructure of *Neopanorpa lipingensis*

The mature spermatozoa of *N. lipingensis* are elongated and filiform, approximately 1300  $\mu\text{m}$  in length, and closely resemble those of *N. lui* in structure, also consisting of a short head, a neck region, and a long posterior flagellum.

The acrosome of mature spermatozoa is also a bilayered structure, consisting of the peripheral acrosomal vesicle and the central perforatorium (Fig. 8H). The nucleus shows a helical appearance (Fig. 8A),  $\sim 0.34 \mu\text{m}$  in diameter. It has two lateral grooves too, assuming a mushroom shape in cross-section (Fig. 8E). The nucleus chromatin is less condensed in the groove, and contains a series of parallel, regularly-spaced septa (Fig. 8B).

The centriole inserts into the basal region of the nucleus (Fig. 8I). Beneath the centriole is an electron-dense centriolar adjunct, which fills most of the volume of the neck region and is on the periphery of the flagellum (Fig. 8C–E).

The flagellum is helical along its entire length (Fig. 8E), and comprises an axoneme, two mitochondrial derivatives, one accessory body, and a pair of extra-axonemal accessory structures. The axoneme has a 9+2 microtubular pattern (Fig. 8E–G) along most of its length. The two mitochondrial derivatives are of unequal size. One is short, thin, and disappears first. The other is prominent, present along most of the remaining length of the flagellum and exhibits a spoon shape in cross-section (Fig. 8E,G).

In the posterior region the flagellum is composed mainly of an axoneme, one mitochondrial derivative, and two accessory structures. At the terminal portion of the flagellum, the microtubules of the axoneme become disorganized and the mitochondrial derivative decreases in size and assumes an elliptical shape in cross-section (Fig. 8J). Furthermore, the spermatozoa show a plasma membrane with a regular glycocalyx composed of longitudinal ridges projecting from the cell membrane (Fig. 8J).



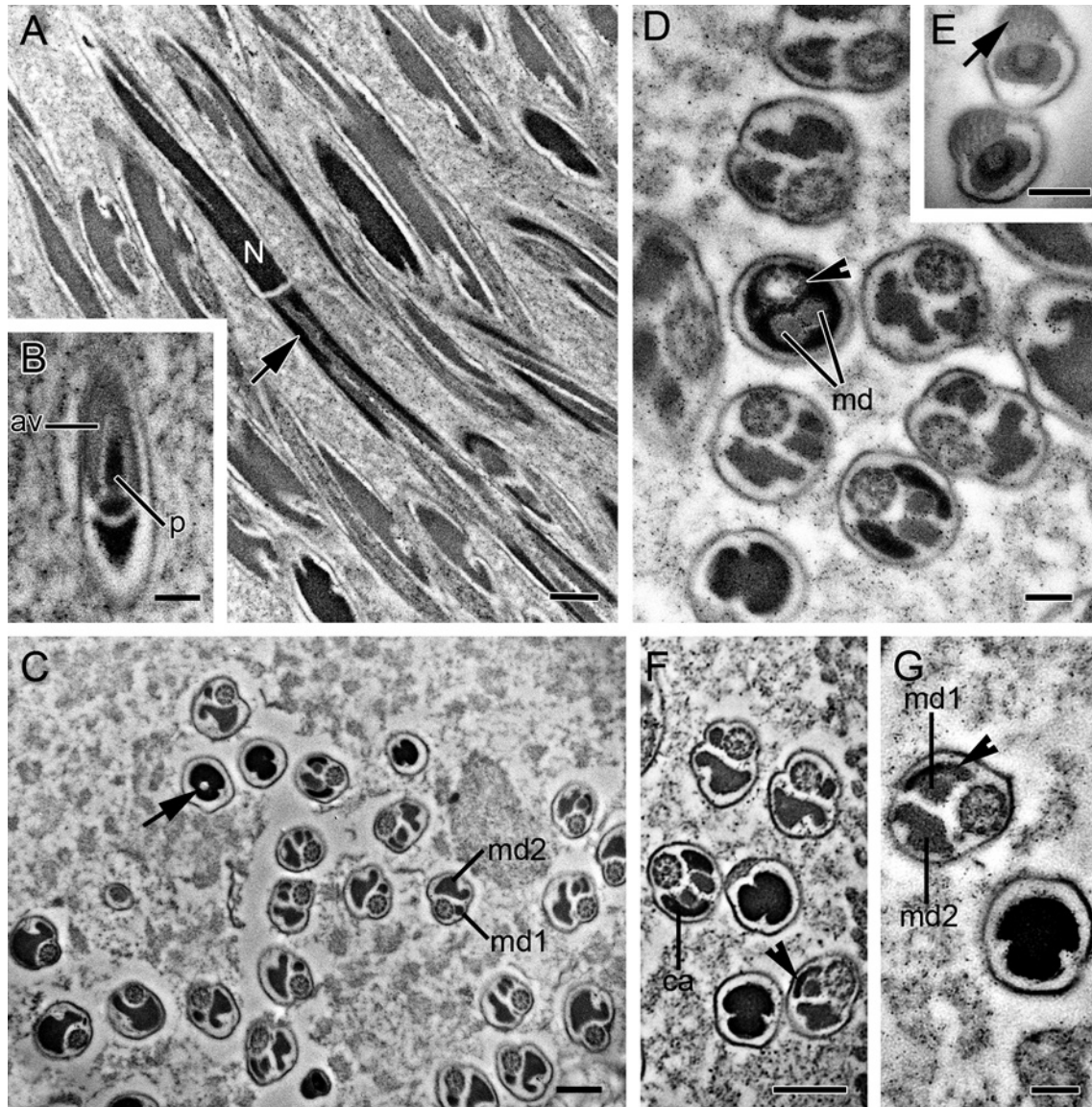


**Fig. 7.** *Neopanorpa lui* Chou & Ran, 1981: spermatozoa, TEM micrographs. **A:** Longitudinal section of the spermatozoa, showing the nucleus (N), centriolar adjunct (arrow) and flagellum. **B:** Longitudinal section of the acrosome with the acrosomal vesicle (av) and perforatorium (p). **C:** Cross-section of the spermatozoa, showing the centriole (arrow) and mitochondrial derivatives (md1, md2). **D:** Magnification of the centriole (arrowhead) and two mitochondrial derivatives (md). **E:** Terminal part of the flagellum with disordered microtubules (arrow) and elliptical mitochondrial derivative. **F, G:** Cross-sections of the flagellum, showing the centriolar adjunct (ca) and the accessory body (arrowheads) in the posterior region. (Scale bars: A, C, F: 0.5  $\mu$ m; B, D, E, G: 0.2  $\mu$ m)

### 3.4. List of characters of sperm

- 01: Glycocalyx: absent (0); present (1).** The glycocalyx of sperm is absent in Micropterigidae (Lepidoptera) (HAMON & CHAUVIN 1992; JAMIESON et al. 1999), but is present in Hepialidae (Lepidoptera); Pulicidae (Siphonaptera); Bittacidae, Boreidae, Panorpidae, and Panorpididae (Mecoptera) (DALLAI et al. 2003; RUSSELL et al. 2013; SHEPARDSON et al. 2014; ZHANG & HUA 2014; ZHANG et al. 2016).
- 02: Type of glycocalyx: structureless (0); transversal ridges (1); longitudinal ridges (2).** The glycocalyx of sperm is composed of longitudinal ridges projecting from the cell membrane in all mecopteran taxa (DALLAI et al. 2003; RUSSELL et al. 2013; SHEPARDSON

- et al. 2014; ZHANG & HUA 2014; ZHANG et al. 2016), and composed of transversal ridges in Pulicidae (DALLAI et al. 2003), but is structureless in Hepialidae (HAMON & CHAUVIN 1992; JAMIESON et al. 1999).
- 03: Acrosome: present (0); absent (1).** The acrosome of sperm is absent in Micropterigidae and Hepialidae in Lepidoptera (HAMON & CHAUVIN 1992; JAMIESON et al. 1999).
- 04: Type of acrosome: bilayered (0); monolayered (1).** The acrosome of sperm is monolayered in Chironomidae and Limoniidae in Diptera (DALLAI et al. 2007, 2008), but is bilayered in Pulicidae and Mecoptera (DALLAI et al. 2003; RUSSELL et al. 2013; SHEPARDSON et al. 2014; ZHANG & HUA 2014; ZHANG et al. 2016).



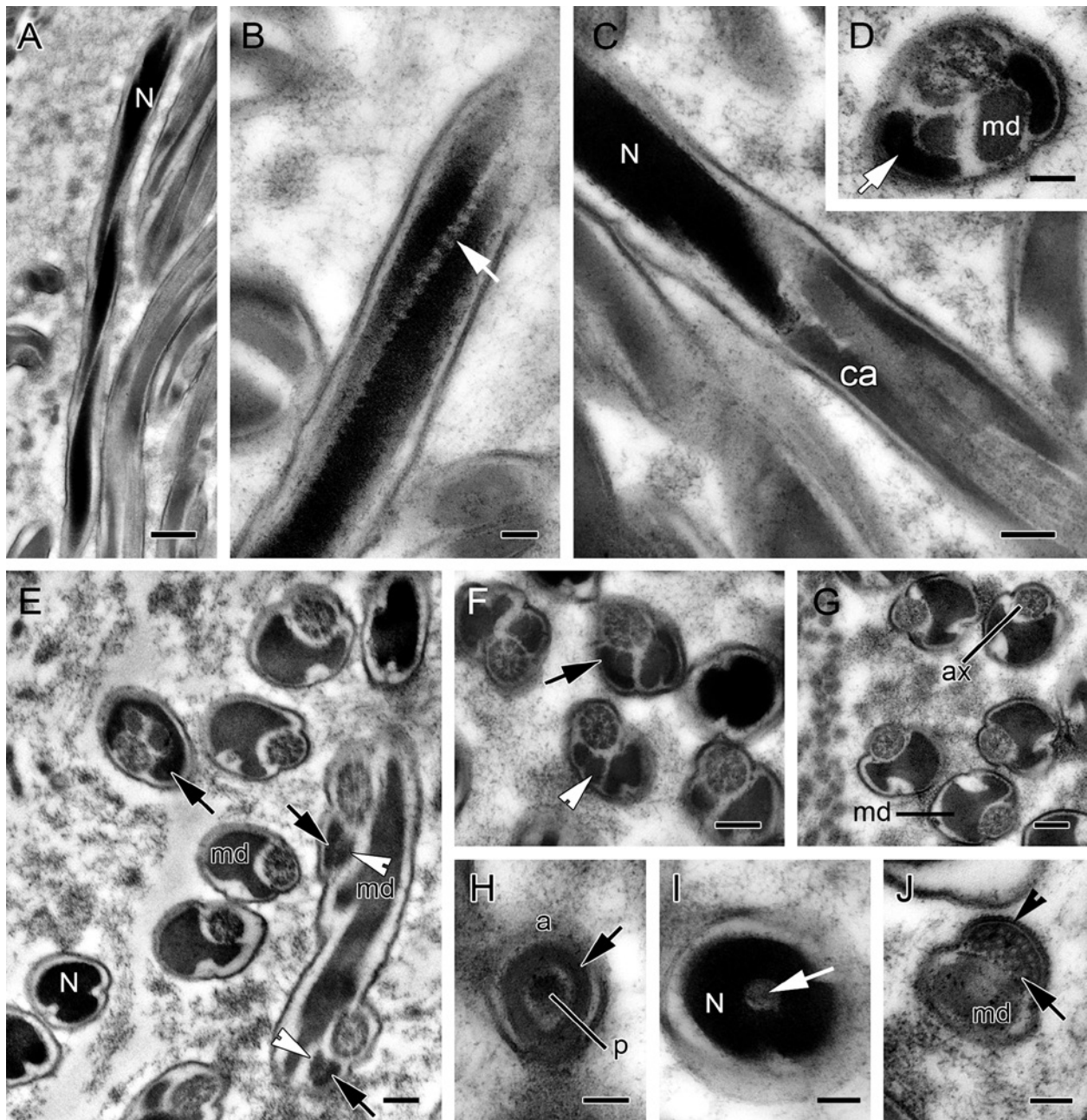


**Fig. 8.** *Neopanorpa lipingensis* Cai & Hua, 2009: spermatozoa, TEM micrographs. **A,B:** Longitudinal sections of the nucleus (N). Arrow points to the regularly-spaced septa in the groove. **C:** Longitudinal section at the neck region, showing the nucleus (N) and centriolar adjunct (ca). **D:** Cross-section at the neck region, showing the centriolar adjunct (arrow) and the two mitochondrial derivatives (md). **E:** Cross- and longitudinal sections of spermatozoa, showing the nucleus (N) with two lateral grooves, the neck region with conspicuous centriolar adjunct (arrow), and the posterior part of flagellum with an axoneme (ax) and a larger mitochondrial derivative (md); arrowheads point to the smaller mitochondrial derivative. **F:** Cross-section at the neck region, showing the axoneme, centriolar adjunct (arrow), the smaller mitochondrial derivative (arrowhead), and the larger mitochondrial derivative. **G:** Cross-section of the posterior part of flagellum, showing the axoneme (ax) and the mitochondrial derivative (md). **H:** Cross-section of the acrosome (a), showing the outer acrosomal vesicle (arrow) and the central perforatorium (p). **I:** Cross-section of the centriole (arrow) inserted into the nucleus (N). **J:** Terminal part of flagellum, showing the irregular microtubules (arrow) and the elliptical mitochondrial derivative (md) in cross-section; arrowhead points to the plasma membrane with the glycocalyx. (Scale bars: A: 0.5  $\mu$ m; B, D, H–J: 0.1  $\mu$ m; C, E–G: 0.2  $\mu$ m)

**05: Length of acrosome: short (0); long (1).** The sperm acrosome is long in Pulicidae for the proportion of acrosome to head larger than 80% (DALLAI et al. 2003).

**06: Length of nucleus: short (0); long (1).** The sperm nucleus is short in Pulicidae for the proportion of nucleus to head smaller than 20% (DALLAI et al. 2003).

**07: Lateral grooves of nucleus: absent (0); present (1).** The grooves of nucleus are absent in Micropterigidae, Hepialidae (HAMON & CHAUVIN 1992; JAMIESON et al. 1999), and Pulicidae (DALLAI et al. 2003).

**08: Number of lateral grooves on nucleus: two (0); three (1).** Two lateral grooves on nucleus occur in Chironomidae (DALLAI et al. 2007) and in all meco-



**Table 1.** Morphological characters and character states used in the cladistic analysis.

Order	Family	0 1	0 2	0 3	0 4	0 5	0 6	0 7	0 8	0 9	1 0	1 1	1 2	1 3	1 4	1 5	1 6	1 7	1 8	1 9	2 0	2 1	2 2
Lepidoptera	Micropterigidae	0	—	1	—	—	1	0	—	—	1	1	1	0	0	0	0	0	0	1	[012]	?	0
	Hepialidae	1	0	1	—	—	1	0	—	—	0	0	0	1	0	0	0	1	0	0	—	—	0
Diptera	Chironomidae	?	?	0	1	0	1	1	0	0	0	1	1	1	[01]	0	0	0	0	0	—	—	0
	Limoniidae	?	?	0	1	0	1	1	[01]	0	0	0	?	1	[02]	1	—	0	0	0	—	—	0
Siphonaptera	Pulicidae	1	1	0	0	1	0	0	—	—	0	0	1	0	0	0	1	0	1	1	0	1	0
Mecoptera	Bittacidae	1	2	0	0	0	1	1	0	1	0	1	1	0	0	0	1	0	1	1	0	1	1
	Boreidae	1	2	0	0	0	1	1	0	1	0	0	0	0	0	0	0	0	1	1	0	0	1
	Panorpidae	1	2	0	0	0	1	1	0	0	1	1	1	0	0	0	1	1	1	1	1	—	1
	Panorpididae	1	2	0	0	0	1	1	0	0	1	0	1	1	0	0	1	1	1	1	0	1	1

pteran taxa (DALLAI et al. 2003; RUSSELL et al. 2013; SHEPARDSON et al. 2014; ZHANG & HUA 2014; ZHANG et al. 2016), but three or two in Limoniidae (DALLAI et al. 2008).

- 09: Depth of grooves on nucleus: deep (0); shallow (1).** The depth of the grooves is shallow in Bittacidae and Boreidae of Mecoptera (DALLAI et al. 2003; RUSSELL et al. 2013; SHEPARDSON et al. 2014).
- 10: Nuclear fiber: absent (0); present (1).** The nuclear fiber of sperm is present in Micropterigidae (HAMON & CHAUVIN 1992; JAMIESON et al. 1999), Panorpidae, and Panorpididae (DALLAI et al. 2003; ZHANG & HUA 2014; ZHANG et al. 2016).
- 11: Nucleus array: non-helical (0); helical (1).** The nucleus is helical in Micropterigidae (HAMON & CHAUVIN 1992; JAMIESON et al. 1999), Chironomidae (DALLAI et al. 2007), Bittacidae, and Panorpidae (DALLAI et al. 2003; SHEPARDSON et al. 2014; ZHANG et al. 2016).
- 12: Flagellum array: non-helical (0); helical (1).** The helical flagellum is present in Micropterigidae (HAMON & CHAUVIN 1992; JAMIESON et al. 1999), Chironomidae (DALLAI et al. 2007), Pulicidae (DALLAI et al. 2003), Bittacidae, Panorpidae and Panorpididae (DALLAI et al. 2003; SHEPARDSON et al. 2014; ZHANG & HUA 2014; ZHANG et al. 2016).
- 13: Nine accessory microtubules of the axoneme: absent (0); present (1).** Accessory microtubules of the axoneme are missing in Micropterigidae (HAMON & CHAUVIN 1992; JAMIESON et al. 1999), Pulicidae (DALLAI et al. 2003), and mecopteran taxa except Panorpididae (DALLAI et al. 2003; RUSSELL et al. 2013; SHEPARDSON et al. 2014; ZHANG et al. 2016).
- 14: Number of central singlet of axoneme: two (0); zero (1); one (2).** The 9+9+0 and 9+9+2 patterns occur in Chironomidae (DALLAI et al. 2007), and 9+9+1 and 9+9+2 patterns occur in Limoniidae (DALLAI et al. 2008).
- 15: Number of mitochondrial derivatives: two (0); one (1).** Only one mitochondrial derivative occurs in Limoniidae (DALLAI et al. 2008), and two are present in remaining groups.
- 16: Relative size of the two mitochondrial derivatives: equal (0); different (1).** Asymmetric mitochondrial derivatives occur in Pulicidae, and also in Bittacidae,

Panorpidae, and Panorpididae (DALLAI et al. 2003; RUSSELL et al. 2013; SHEPARDSON et al. 2014; ZHANG & HUA 2014; ZHANG et al. 2016).

- 17: Transverse section of the mitochondrial derivative: regular (0); irregular (1).** The irregular shape of the transverse section with projection is present in Hepialidae (HAMON & CHAUVIN 1992; JAMIESON et al. 1999), Panorpidae, and Panorpididae (DALLAI et al. 2003; ZHANG & HUA 2014; ZHANG et al. 2016).
- 18: Crystalline structure of the mitochondrial derivative: absent (0); present (1).** The crystalline structure of the mitochondrial derivative is present in Pulicidae, and all mecopteran taxa (DALLAI et al. 2003; RUSSELL et al. 2013; SHEPARDSON et al. 2014; ZHANG & HUA 2014; ZHANG et al. 2016).
- 19: Accessory bodies: absent (0); present (1).** Accessory bodies are absent in Hepialidae (HAMON & CHAUVIN 1992; JAMIESON et al. 1999), Chironomidae, and Limoniidae (DALLAI et al. 2007, 2008).
- 20: Number of accessory bodies: two (0); one (1); three (2).** The number of accessory bodies ranges from one to three in Micropterigidae (HAMON & CHAUVIN 1992; JAMIESON et al. 1999), but is one in Panorpidae (DALLAI et al. 2003; ZHANG et al. 2016), two in the remaining taxa.
- 21: Relative size of accessory bodies: equal (0); different (1).** Asymmetric accessory bodies occur in Pulicidae, Bittacidae, and Panorpididae (DALLAI et al. 2003; RUSSELL et al. 2013; SHEPARDSON et al. 2014; ZHANG & HUA 2014).
- 22: Extra-axonemal accessory structures/rods: absent (0); present (1).** These structures were only observed in the sperm flagellum of the mecopteran taxa (DALLAI et al. 2003; RUSSELL et al. 2013; SHEPARDSON et al. 2014; ZHANG & HUA 2014; ZHANG et al. 2016).

### 3.5. Phylogenetic analysis

The phylogenetic analysis yielded one most parsimonious tree [branch length = 31, consistency index (CI) = 0.68, retention index (RI) = 0.63], which supports closer affinities of Siphonaptera and the mecopteran clade comprising Panorpidae, Panorpididae, Bittacidae, and Boreidae. The most parsimonious tree with unambiguous char-

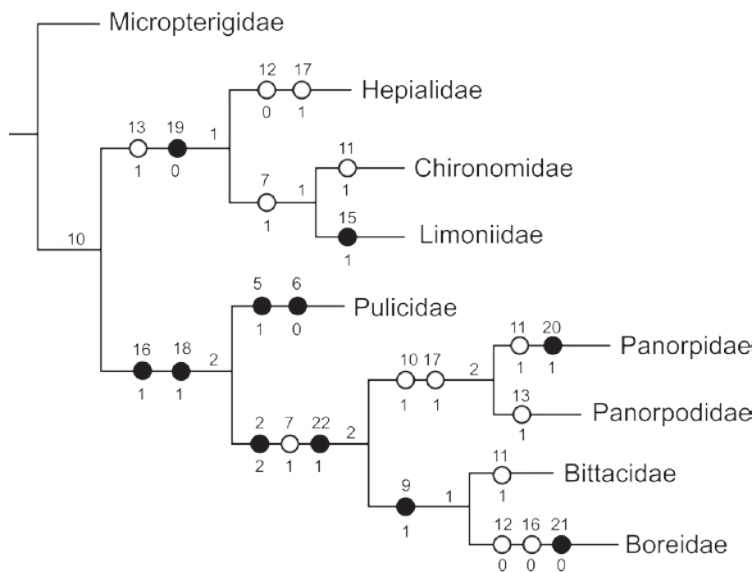


**Fig. 9.** The most parsimonious tree with Micropterigidae and Hepialidae (Lepidoptera) as outgroup taxa. Bremer support values are indicated at internal nodes. Non-homoplasious characters are marked with filled circles and homoplasious characters with open circles. The numbers and states of characters are placed above and below the circles, respectively.

acters is shown in Figure 9. According to the topology of the cladogram, all the mecopteran taxa (Panorpidae, Panorpididae, Bittacidae, and Boreidae) form a monophyletic group, which is the sister group of Pulicidae (Siphonaptera). The mecopteran clade and Siphonaptera, in turn, constitute the sister group of Diptera. The sister group relationship between the mecopteran clade and Siphonaptera is supported by two non-homoplasious characters: two asymmetric mitochondrial derivatives (character 16: 1) and the mitochondrial derivative with crystalline structure (character 18: 1). The monophyly of the mecopteran taxa (Panorpidae, Panorpididae, Bittacidae, and Boreidae) is supported (Bremer support value = 2) by two non-homoplasious apomorphies: glycocalyx organised in longitudinal ridges (character 2: 2) and two extra-axonemal accessory structures/rods (character 22: 1). In Mecoptera, Panorpidae and Panorpididae receive a support (Bremer support value = 2) as sister taxa, although they are characterized only by two homoplasious apomorphies: presence of nuclear fiber (character 10: 1) and irregular transverse section of mitochondrial derivative (character 17: 1).

#### 4. Discussion

The sperm ultrastructures are very similar between the two species of *Neopanorpa* and share the following characters with the confamilial *Panorpa* and *Furcatopanorpa*: a short bilayered acrosome, a helical elongated nucleus with two lateral longitudinal grooves, a neck region with the prominent centriolar adjunct, and a long helical flagellum composed of a 9+2 axoneme, two mitochondrial derivatives of unequal size, one accessory body, and two extra-axonemal accessory structures (DALLAI et al. 2003; DALLAI 2014; ZHANG et al. 2016). The diagnostic character of the *Neopanorpa* sperm lies in the speci-

cally spoon-shaped mitochondrial derivative along most of the flagellum length.

The notable feature of *Neopanorpa* sperm lies in the peculiar shape of the mitochondrial derivative in the posterior portion of the flagellum. The mitochondrial derivatives are transformed by the conspicuous interlocked structure “nebenkern”, which is formed by numerous mitochondria aggregated and fused in the cytoplasm of spermatids. The two mitochondrial derivatives of mature spermatozoa are unequal in size. One is thin and short, and the other is prominent and extends along the entire length of the flagellum. The larger mitochondrial derivative assumes an irregular shape in cross-section for most length of the tail. This irregular condition was also found in *Panorpa annexa* and *P. nuptialis* (crescentic-shaped) and *Furcatopanorpa longihypovalva* (hammer-shaped) of Panorpidae (GASSNER et al. 1972; JAMIESON et al. 1999; ZHANG et al. 2016), and *Panorpodes kuandianensis* (anchor-shaped) of Panorpididae (ZHANG & HUA 2014). In other families of Mecoptera the mitochondrial derivatives of flagellum are relatively regular in cross-section: circular in Bittacidae and elliptical in Boreidae (DALLAI et al. 2003; RUSSELL et al. 2013; SHEPARDSON et al. 2014). The mitochondrial derivatives differ among the four studied families (Bittacidae, Boreidae, Panorpidae, and Panorpididae), indicating that the mitochondrial derivatives likely provide useful characters in the phylogenetic analysis of Mecoptera.

During spermiogenesis the spermatids are usually surrounded by microtubules (or microtubular manchette) in most Hexapoda (JAMIESON et al. 1999; DALLAI 2014). The microtubules vary in number and arrangement from group to group or from species to species (FOLLIOU & MAILLET 1970; DANILOVA et al. 1984; DALLAI et al. 2002, 2004; CHAWANJI et al. 2007). The transient microtubules only exist in the deformation process of spermatids, and disappear in mature spermatozoa (JAMIESON et al. 1999; DALLAI 2014). During the spermiogenesis of *Neopanorpa*, the spermatid components, including the nucleus



and mitochondrial derivatives, are visibly surrounded by a single layer of microtubules, which disappear in the mature spermatozoa. This may confirm the role of microtubules in the spermatid elongation in the spermiogenesis.

The lateral laminae are a pair of peculiar structures alongside the two lateral grooves of the nuclear envelope in the spermatids during the spermiogenesis. The lateral laminae are present and remain parallel to the nucleus of spermatozoa of *Panorpa germanica* (DALLAI et al. 2003), but are absent in the mature spermatozoa of *Bittacus* (SHEPARDSON et al. 2014). Based on our present investigation, the lateral laminae of *Neopanorpa* are similar to those of *Bittacus*, only present during the deformation process of spermatids and absent in the mature spermatozoa, suggesting that the lateral laminae are likely related to nuclear twisting.

WHITING (2002) argued that Mecoptera (Boreidae) is paraphyletic with Siphonaptera based on DNA sequence data. Other authors (WIEGMANN et al. 2009; BEUTEL et al. 2011; MISOF et al. 2014), however, regarded Mecoptera as a monophyletic group based on both morphological characters and molecular data. Based on our preliminary phylogenetic analysis from 22 characters of sperm ultrastructure (Fig. 9), two non-homoplasious characters (glycocalyx organised in longitudinal ridges and two extra-axonemal accessory structures/rods) support the clade comprising all the taxa (Panorpidae, Panorpodidae, Bittacidae, and Boreidae) studied of Mecoptera, and reject the sister group relationship of Boreidae with Siphonaptera. This conclusion conforms to the viewpoints of DALLAI et al. (2003) and RUSSELL et al. (2013). In addition, two non-homoplasious characters (two asymmetric mitochondrial derivatives and mitochondrial derivative with crystalline structure) support the sister group relationship of Siphonaptera and the mecopteran clade in our tentative phylogenetic analysis based on the existing data, although the sperm information of some crucial taxa like Nannochoristidae is unavailable. This sister group relationship conforms with GOTTARDO et al. (2016). Based on the limited number of characters available, our analysis shows that the sister taxon of Panorpodidae is Panorpidae, instead of Bittacidae as viewed by WHITING (2002).

Possibly due to the technique complexity and difficulty of transmission electron microscopy, only limited numbers of insects have been investigated for their sperm ultrastructure so far. Admittedly, our present phylogenetic analysis of Mecoptera was only conducted on the basis of very limited existing data of sperm ultrastructure. On the other hand, the taxon sampling, including the ingroups, was also limited to the taxa whose sperm structures have been studied in Antliophora. In this case, only one family (Pulicidae) was selected in Siphonaptera. Although it is widely accepted that Nannochoristidae is a crucial taxon in the phylogenetic analysis of Mecoptera (BEUTEL & BAUM 2008; WIEGMANN et al. 2009; BEUTEL et al. 2011), the data of sperm ultrastructure are unfortunately unavailable yet. The aforementioned conclusion is only

putative to a large extent. To obtain a robust phylogenetic analysis of Mecoptera, molecular data should be considered in combination with other morphological characters as well as sperm ultrastructure.

## 5. Acknowledgments

We thank Ying Miao for assistance in specimen collection, Xiao-Hua He for assistance in transmission electron microscopy, and Victor Benno Meyer-Rochow for critical review on the early draft of the manuscript. This study was supported by the National Natural Science Foundation of China (grant no. 31672341) and the Scientific Research Foundation of Hainan University (grant no. KYQD (ZR) 1705).

## 6. References

- BACCETTI B. 1972. Insect sperm cells. – *Advances in Insect Physiology* **9**: 315–397.
- BEUTEL R.G., BAUM E. 2008. A longstanding entomological problem finally solved? Head morphology of *Nannochorista* (Mecoptera, Insecta) and possible phylogenetic implications. – *Journal of Zoological Systematics and Evolutionary Research* **46**: 346–367.
- BEUTEL R.G., FRIEDRICH F., HÖRNSCHEMEYER T., POHL H., HÜNEFELD F., BECKMANN F., MEIER R., MISOF B., WHITING M.F., VILHELMSEN L. 2011. Morphological and molecular evidence converge upon a robust phylogeny of the megadiverse Holometabola. – *Cladistics* **27**: 341–355.
- BIRKHEAD T.R., HOSKEN D.J., PITNICK S. 2009. *Sperm Biology: An Evolutionary Perspective*. – Elsevier, London. 642 pp.
- BREMER K. 1994. Branch support and tree stability. – *Cladistics* **10**: 295–304.
- BYERS G.W., THORNHILL R. 1983. Biology of the Mecoptera. – *Annual Review of Entomology* **28**: 203–228.
- CAI L.J., HUA B.Z. 2009. A new *Neopanorpa* (Mecoptera, Panorpidae) from China with notes on its biology. – *Deutsche Entomologische Zeitschrift* **56**: 93–99.
- CAI L.J., HUANG P.Y., HUA B.Z. 2008. *Sinopanorpa*, a new genus of Panorpidae (Mecoptera) from the Oriental China with descriptions of two new species. – *Zootaxa* **1941**: 43–54.
- CHAWANJI A.S., HODGSON A.N., VILLET M.H., SANBORN A.F., PHILLIPS P.K. 2007. Spermiogenesis in three species of cicadas (Hemiptera: Cicadidae). – *Acta Zoologica* **88**: 337–348.
- CHEN Q.X., LI T., HUA B.Z. 2012. Ultrastructure of the larval eye of the scorpionfly *Panorpa dubia* (Mecoptera: Panorpidae) with implications for the evolutionary origin of holometabolous larvae. – *Journal of Morphology* **273**: 561–571.
- CHOU I., RAN R.B., WANG S.M. 1981. Taxonomic studies on the Chinese Mecoptera (I, II). – *Entomotaxonomia* **3**: 1–22.
- DALLAI R. 2009. The contribution of the sperm structure to the reconstruction of the hexapod phylogeny. – *Proceedings of the Arthropodan Embryological Society of Japan* **43**: 23–38.
- DALLAI R. 2014. Overview on spermatogenesis and sperm structure of Hexapoda. – *Arthropod Structure & Development* **43**: 257–290.
- DALLAI R., LUPETTI P., CAREPELLI A., FRATI F., AFZELIUS B.A. 2002. Sperm structure and spermiogenesis in *Atelura formicaria* Heyden (Zygentoma, Insecta). – *Acta Zoologica* **83**: 245–262.
- DALLAI R., LUPETTI P., AFZELIUS B.A., FRATI F. 2003. Sperm structure of Mecoptera and Siphonaptera (Insecta) and the phylo-

- genetic position of *Boreus hyemalis*. – *Zoomorphology* **122**: 211–220.
- DALLAI R., CAREPELLI A., NARDI F., FANCIULLI P.P., LUPETTI P., AFZELIUS B.A., FRATI F. 2004. Sperm structure and spermiogenesis in *Coletinia* sp. (Nicoletiidae, Zygentoma, Insecta) with a comparative analysis of sperm structure in *Zygentoma*. – *Tissue & Cell* **36**: 233–244.
- DALLAI R., LOMBARDO B.M., LUPETTI P. 2007. Sperm ultrastructure in Chironomoidea (Insecta, Diptera). – *Tissue & Cell* **39**: 179–194.
- DALLAI R., LOMBARDO B.M., MERCATI D., VANIN S., LUPETTI P. 2008. Sperm structure of Limoniidae and their phylogenetic relationship with Tipulidae (Diptera, Nematocera). – *Arthropod Structure & Development* **37**: 81–92.
- DALLAI R., GOTTARDO M., BEUTEL R.G. 2016. Structure and evolution of insect sperm: new interpretations in the age of phylogenomics. – *Annual Review of Entomology* **61**: 1–23.
- DANILOVA L.V., GABER E.S., SHINYAEVA L.I. 1984. Spermiogenesis and the ultrastructure of mature sperm in *Eurygaster intergriiceps*. – *Gamete Research* **9**: 75–86.
- FOLLIOU R., MAILLET P.L. 1970. Ultrastructure de la spermiogenèse et du spermatozoïde de divers insectes Homoptères. Pp. 289–300 in: BACCETTI B. (ed.), *Comparative Spermatology*. – Academic Press, New York.
- FRIEDRICH F., POHL H., BECKMANN F., BEUTEL R.G. 2013. The head of *Merope tuber* (Meropeidae) and the phylogeny of Mecoptera (Hexapoda). – *Arthropod Structure & Development* **42**: 69–88.
- GAO C., MA N., HUA B.Z. 2016. *Cerapanorpa*, a new genus of Panorpidae (Insecta: Mecoptera) with descriptions of three new species. – *Zootaxa* **4158**: 93–104.
- GASSNER G., BRELAND O.P., BIESLE J.J. 1972. The spermatozoa of the scorpionfly *Panorpa nuptialis*: a transmission electron microscope study. – *Annals of the Entomological Society of America* **65**: 1302–1309.
- GOLOBOFF P.A. 1999. NONA ver. 2. Published by the author, Tucuman, Argentina.
- GOLOBOFF P.A., FARRIS J.S., NIXON K.C. 2008. TNT, a free program for phylogenetic analysis. – *Cladistics* **24**: 774–786.
- GOTTARDO M., DALLAI R., MERCATI D., HÖRNSCHEMEYER T., BEUTEL R.G. 2016. The evolution of insect sperm – an unusual character system in a megadiverse group. – *Journal of Zoological Systematics and Evolutionary Research* **54**: 237–256.
- HAMON C., CHAUVIN G. 1992. Ultrastructural analysis of spermatozoa of *Korscheltellus lupulinus* L. (Lepidoptera: Hepialidae) and *Micropterix calthella* L. (Lepidoptera: Micropterigidae). – *International Journal of Insect Morphology and Embryology* **21**: 149–160.
- HU G.L., YAN G., XU H., HUA B.Z. 2015. Molecular phylogeny of Panorpidae (Insecta: Mecoptera) based on mitochondrial and nuclear genes. – *Molecular Phylogenetics and Evolution* **85**: 22–31.
- JAMIESON B.G.M. 1987. *The Ultrastructure and Phylogeny of Insect Spermatozoa*. – Cambridge University Press, Cambridge. 320 pp.
- JAMIESON B.G.M., DALLAI R., AFZELIUS B.A. 1999. *Insects: Their Spermatozoa and Phylogeny*. – Scientific Publishers, Enfield. 555 pp.
- KALTENBACH A. 1978. Mecoptera (Schnabelhafte, Schnabelfliegen). – *Handbuch der Zoologie* **4**(2); (2/28): 1–111.
- KRISTENSEN N.P. 1999. Phylogeny of endopterygote insects, the most successful lineage of living organisms. – *European Journal of Entomology* **96**: 237–253.
- LINNAEUS C. 1758. *Systema natura per regna tria naturae secundum classes, ordines, genera, species, cum characteribus, differentiis, synonymis, locis*. 10<sup>th</sup> Edn. Vol. 1. – Salvii, Holmiae. 824 pp.
- MA N., HUA B.Z. 2011. *Furcatopanorpa*, a new genus of Panorpidae (Mecoptera) from China. – *Journal of Natural History* **45**: 2251–2261.
- MACLACHLAN R. 1875. A sketch of our present knowledge of the neuropterous fauna of Japan (excluding Odonata and Trichoptera). – *Transactions of the Entomological Society of London* **1875**: 167–190.
- MELZER R.R., PAULUS H.F., KRISTENSEN N.P. 1994. The larval eye of nannochoristid scorpionflies (Insecta, Mecoptera). – *Acta Zoologica* **75**: 201–208.
- MISOF B., LIU S., MEUSEMANN K., et al. 2014. Phylogenomics resolves the timing and pattern of insect evolution. – *Science* **346**: 763–767.
- NIXON K.C. 2002. WinClada ver. 1.00.08. – Published by the author, Ithaca, NY.
- PENNY N.D., BYERS G.W. 1979. A check-list of the Mecoptera of the world. – *Acta Amazonica* **9**: 365–388.
- RUSSELL L.K., DALLAI R., GOTTARDO M., BEUTEL R.G. 2013. The sperm ultrastructure of *Caurinus dectes* Russell (Mecoptera: Boreidae) and its phylogenetic implications. – *Tissue & Cell* **45**: 397–401.
- SHEPARDSON S.P., HUMPHRIES B.A., PELKKI K.L., STANTON D.J. 2014. Spermatozoon ultrastructure of hangingflies, *Bittacus strigosus* and *Bittacus stigmaterus*. – *Journal of Insect Science* **14**: 10.
- VAN DER WEELE H.W. 1909. Mecoptera and Planipennia of Insulinde. – *Notes from the Leyden Museum* **31**: 1–100.
- WHITING M.F. 2002. Mecoptera is paraphyletic: multiple genes and phylogeny of Mecoptera and Siphonaptera. – *Zoologica Scripta* **31**: 93–104.
- WIEGMANN B.M., TRAUTWEIN M.D., KIM J.W., CASSEL B.K., BERTONE M.A., WINTERTON S.L., YEATES D.K. 2009. Single-copy nuclear genes resolve the phylogeny of the holometabolous insects. – *BMC Biology* **7**: 34.
- WILLMANN R. 1987. The phylogenetic system of the Mecoptera. – *Systematic Entomology* **12**: 519–524.
- ZHANG B.B., HUA B.Z. 2014. Sperm ultrastructure of *Panorposes kuandianensis* (Mecoptera, Panorpididae). – *Microscopy Research and Technique* **77**: 394–400.
- ZHANG B.B., LYU Q.H., HUA B.Z. 2016. Male reproductive system and sperm ultrastructure of *Furcatopanorpa longihypovalva* (Hua and Cai, 2009) (Mecoptera: Panorpidae) and its phylogenetic implication. – *Zoologischer Anzeiger* **264**: 41–46.
- ZHONG W., HUA B.Z. 2013. *Dicerapanorpa*, a new genus of East Asian Panorpidae (Insecta: Mecoptera: Panorpididae) with descriptions of two new species. – *Journal of Natural History* **47**: 1019–1046.



# ZOBODAT - [www.zobodat.at](http://www.zobodat.at)

Zoologisch-Botanische Datenbank/Zoological-Botanical Database

Digitale Literatur/Digital Literature

Zeitschrift/Journal: [Arthropod Systematics and Phylogeny](#)

Jahr/Year: 2017

Band/Volume: [75](#)

Autor(en)/Author(s): Zhang Bei-Bei, Hua Bao-Zhen

Artikel/Article: [Spermatogenesis and sperm structure of Neopanorpa lui and Neopanorpa lipingensis \(Mecoptera: Panorpidae\) with phylogenetic considerations 373-386](#)